Electronic Supplementary Information

Dose-dependent effect of proton irradiation on electrical properties of WSe_2 ambipolar field effect transistors

Jiwon Shin,[a] Kyungjune Cho,[a] Tae-Young Kim,[a§] Jinsu Pak,[a] Jae-Keun Kim,[a] Woocheol lee,[a] Jaeyoung Kim,[a] Seungjun Chung,[b] Woong-Ki Hong,[c] and Takhee Lee*[a]*

[a]Department of Physics and Astronomy, and Institute of Applied Physics, Seoul National University, Seoul 08826, Korea.
E-mail: tlee@snu.ac.kr
[b]Photo-Electronic Hybrids Research Center, Korea Institute of Science and Technology, Seoul 02792, Korea.
[c]Jeonju Center, Korea Basic Science Institute, Jeonju, Jeollabuk-do 54907, Korea
E-mail: wkh27@kbsi.re.kr
[§]Flash Process Architecture Team, Samsung Electronics, 114, Samseong-ro, Pyeongtaek-si, Gyeonggi-do 17786, Korea

Table of Contents

1. Device fabrication

Figure S1 illustrates the device fabrication processes for WSe_2 ambipolar FETs. First, a highly doped p-type Si wafer with 270 nm thick SiO_2 layer was prepared. The WSe_2 flakes were transferred onto the silicon substrate by the mechanical exfoliation using a scotch tape from a bulk WSe_2 crystal (purchased from HQ Graphene). Using an optical microscope, candidate WSe_2 flakes with a few layers thickness range from 4 to 7 nm were selected to make ambipolar type WSe_2 FETs. (Table S1) The thicknesses of WSe_2 flakes were measured using an atomic force microscope (AFM) (Park Systems, NX10). Then, we spin-coated a bi-layer electron beam resist; first methyl methacrylate (MMA) (8.5) MAA (9% concentration in ethyl lactate) was spin-coated on the samples at 4,000 rpm for 50 s, and then the samples were baked on a hotplate at 180 °C for 90 s. Next, poly methyl methacryllate (PMMA) 950K (5% concentration in anisole) was spin-coated on MMA-coated samples at 4,000 rpm for 50 s, followed by a bake on the hotplate at 180 °C for 90 s. Then, we patterned the source and drain electrodes using an electron beam lithography (JEOL, JSM-6510) and performed development process with methyl isobutyl ketone: isopropyl alcohol (MIBK:IPA) (1:3) solution for 50 s. Finally, we deposited Au (40 nm)/Ti (5 nm) as the source and drain electrodes using an electron beam evaporator.

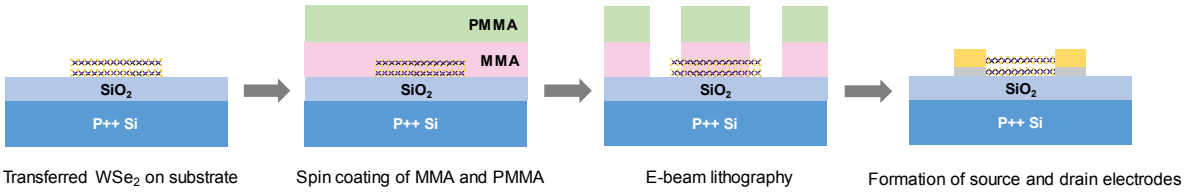

Figure S1. Schematics of WSe_2 device fabrication.

2. Ambipolar characteristics of WSe_2 FETs with various WSe_2 thickness

Figure S2(a)-(c) show the AFM images of WSe_2 flakes and corresponding transfer curves of the WSe_2 FETs. The thickness of WSe_2 flakes were determined as ~5.1, 5.8, and 7 nm, which correspond to 8, 9, and 11 layers (the thickness of single WSe_2 layer is 0.65 nm), respectively. The transfer characteristics (drain-source current versus gate voltage, I_{DS}–V_{GS}) were measured at a fixed drain-source voltage (V_{DS}) of 1 V and showed ambipolar characteristics.

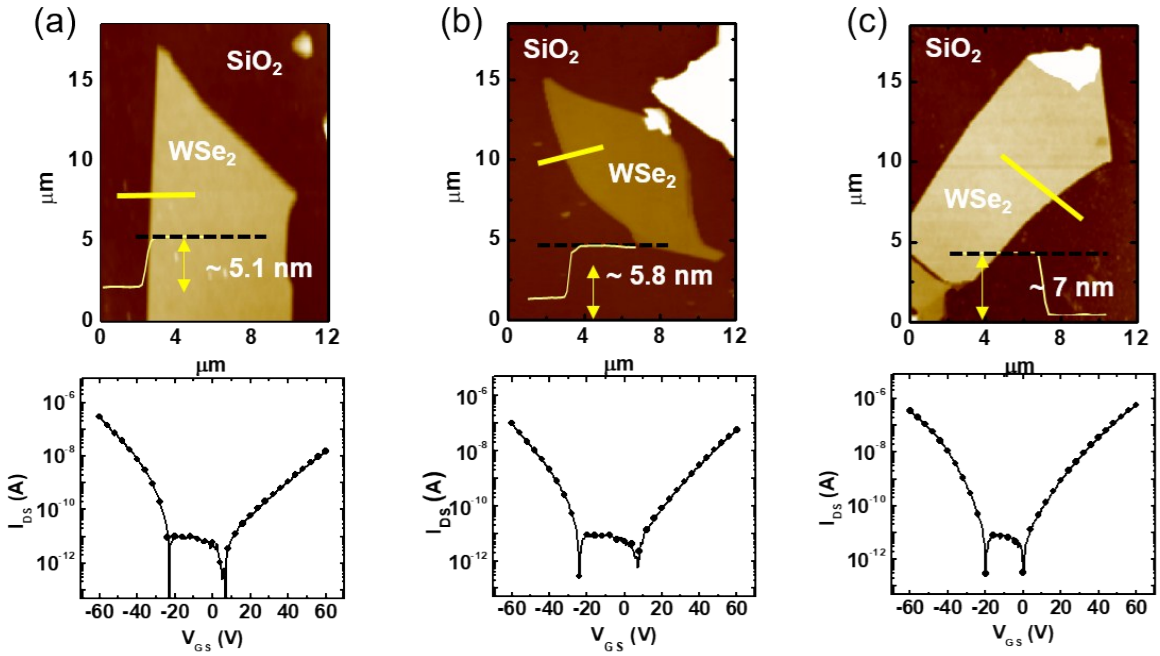

Figure S2. The AFM images of WSe_2 flakes and corresponding transfer curves of the WSe_2 FETs with thickness of (a) 5.1 nm, (b) 5.8 nm, and (c) 7 nm.

3. V_{DS}–I_{DS} for irradiation dose condition of 10^{12}, 10^{13}, 10^{14}, and 10^{15} cm^{-2}

Figure S3 is the output characteristics (drain-source current versus drain-source voltage, I_{DS}–V_{DS}) of before (black open square) and after (red filled circle) proton beam irradiation with the dose conditions of 10^{12}, 10^{13}, 10^{14}, and 10^{15} cm^{-2} for (a) hole and (b) electron accumulation regimes. The output characteristics were measured at fixed gate-source voltages (V_{GS}) of (a) -60 V and (b) 60 V. The current levels in the hole accumulation regime decreased and increased for proton beam-irradiated devices under low dose condition of 10^{12}, 10^{13}, and 10^{14} cm^{-2} and high dose condition of 10^{15} cm^{-2}, respectively. For electron accumulation regime, the current level changed oppositely; it increased and decreased for proton beam-irradiated devices under low dose condition and high dose condition, respectively.

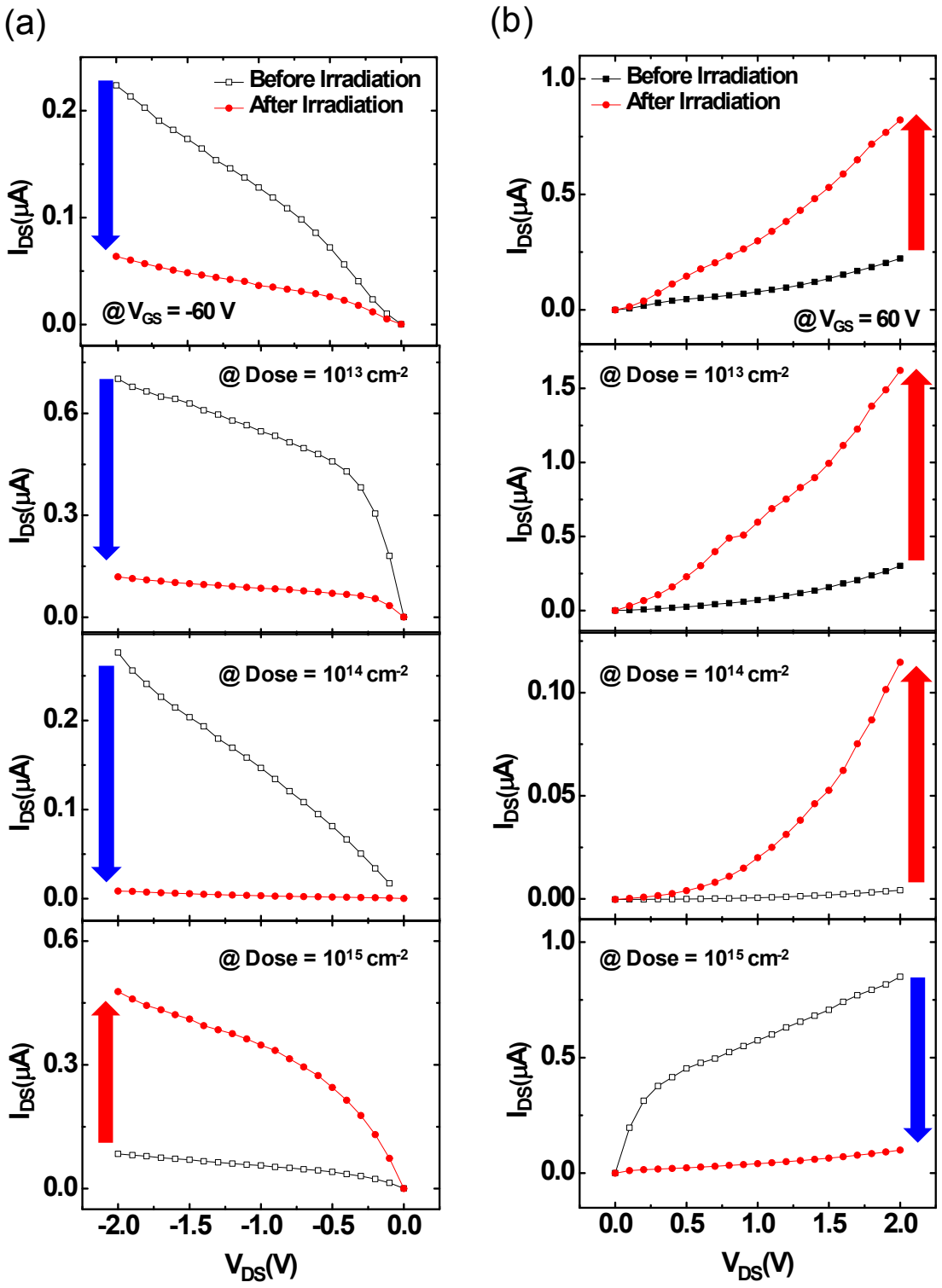

Figure S3. The output characteristics with proton beam irradiation dose conditions of 10^{12}, 10^{13}, 10^{14}, and 10^{15} cm^{-2} for (a) hole and (b) electron accumulation regimes.

4. Subthreshold swing value of the devices before and after the proton irradiation

Figure S4 shows the statistical results of the subthreshold swing (SS) values of the WSe_2 devices for (a) hole and (b) electron accumulation regimes before (black filled squares) and after (red filled circles) proton beam irradiation. 4 to 6 devices for each dose condition were characterized and a total of 20 devices were analyzed. The SS values changed slightly with no clear dependence on the dose condition in both hole and electron accumulation regimes.

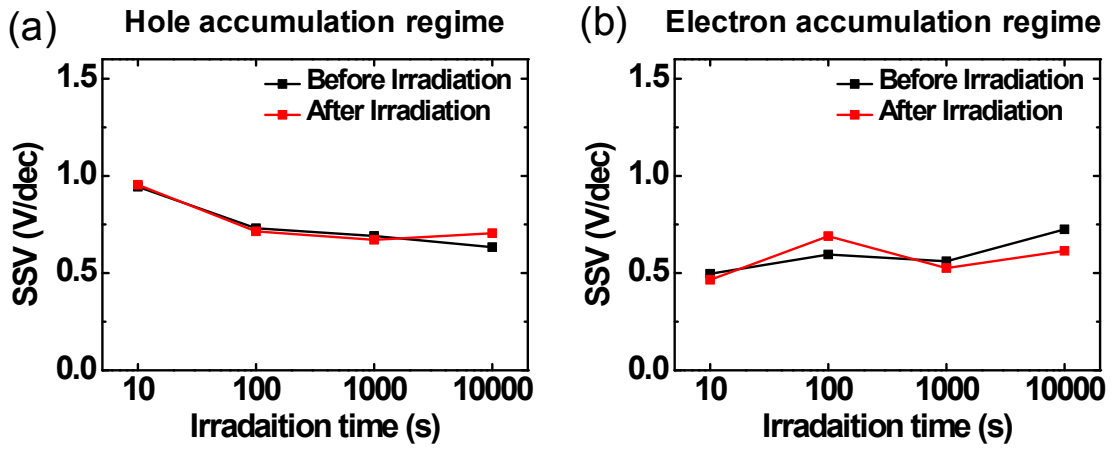

Figure S4. Subthreshold swing value of the devices before and after the proton beam irradiation for (a) hole and (b) electron accumulation regimes.

5. Mobility of the devices before and after the proton beam irradiation

Figure S5 shows the mobility of the WSe_2 devices before and after the proton beam irradiation. The mobility of the ambipolar WSe_2 FET devices was calculated using the following equation:

$$\mu = \frac{L}{W C_i V_{DS}} \frac{1}{dV_{GS}} \frac{dI_{DS}}{}$$

where L and W are the channel length and width of the FET, respectively. V_{DS} is the source−drain voltage. I_{DS} is the current flowing from source to drain, and V_{GS} is the gate voltage. C_i is the gate capacitance per unit area. The mobility values of proton beam-irradiated devices under low dose condition (10^{12}, 10^{13}, and 10^{14} cm^{-2}) are smaller in the hole accumulation regime and larger in the electron accumulation regime compared to those of the pristine devices before proton beam irradiation. The mobility values of proton beam-irradiated devices under high dose condition (10^{15} cm^{-2}) are larger in the hole accumulation regime and smaller in the electron accumulation regime compared to those of the pristine devices before the proton beam irradiation.

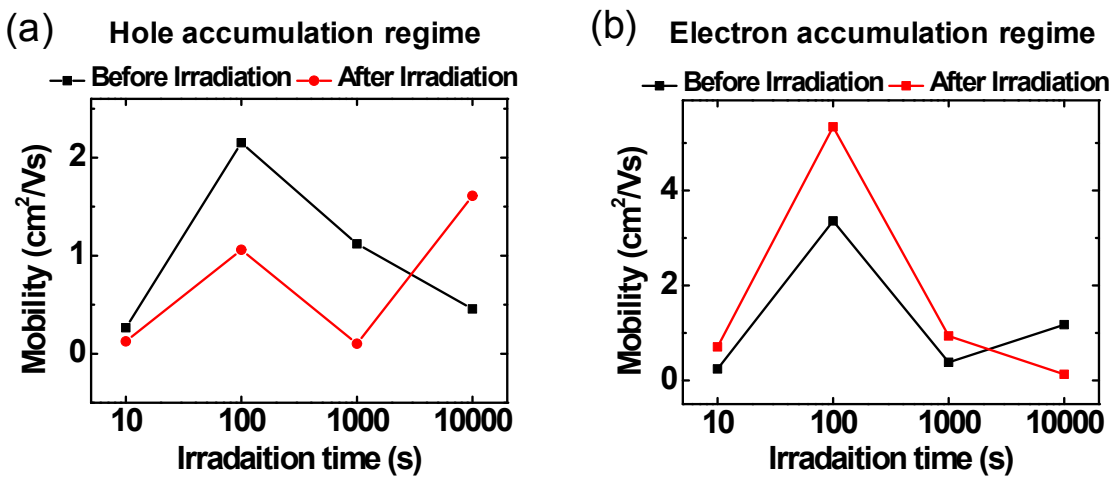

Figure S5. Mobility of the devices before and after the proton beam irradiation for (a) hole and (b) electron accumulation regimes.

6. Stopping and Range of Ions in Matter (SRIM) analysis

We performed simulations of the stopping depth of proton beam using Stopping and Range of Ions in Matter (SRIM) software to understand the behavior of protons.[S2] The structure of our WSe_2 FET devices is WSe_2 (4-7 nm)/SiO_2 (270 nm)/Si (500 μm). We found the protons with 10 nA current and 10 MeV energy deposited most of their energy near 700 μm from the top surface. Some amount of energy can also be transferred to the SiO_2 dielectric layer which creates electron-hole pairs.

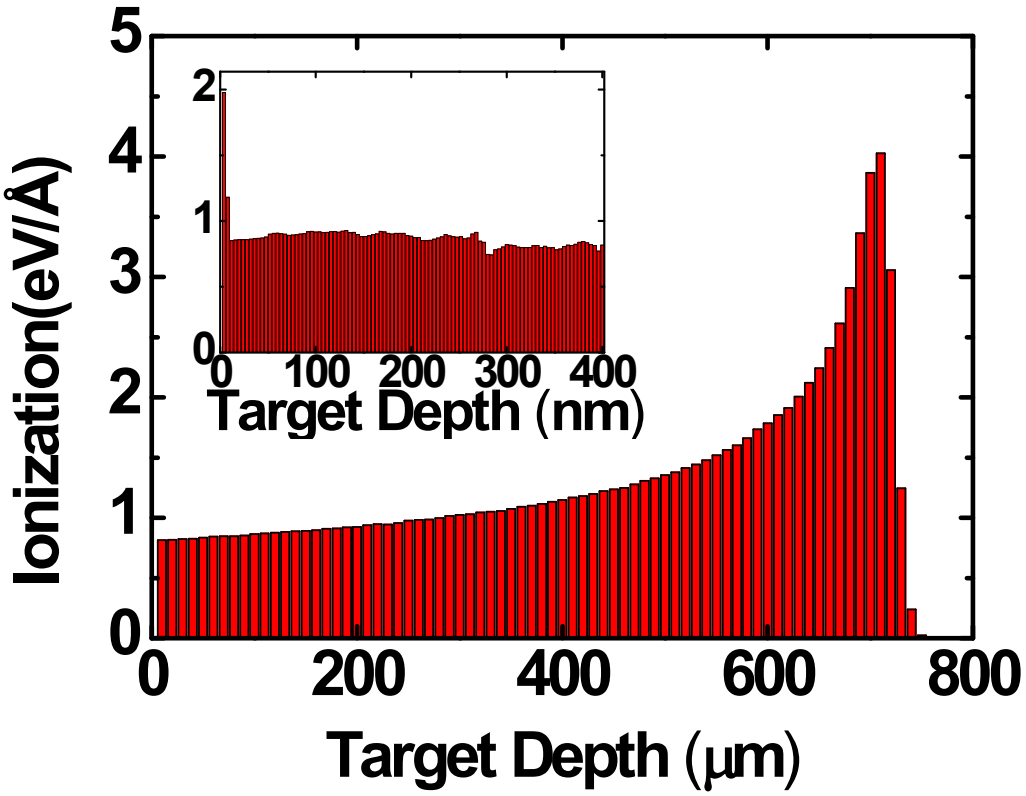

Figure S6. The energy loss profiles of the protons simulated by SRIM. The inset image is a zoomed result for the range of 0-400 nm from the top surface which includes the oxide layer.

7. The I_{GS}–V_{GS} leakage plot of the WSe_2 FET

We measured the gate leakage current of the WSe_2 FET as shown in Figure S6. The leakage current was found small enough compared to the signal current. In case of I_{GS} which was measured without pre-amplifier, the measurement limit was 10^{-10} A.

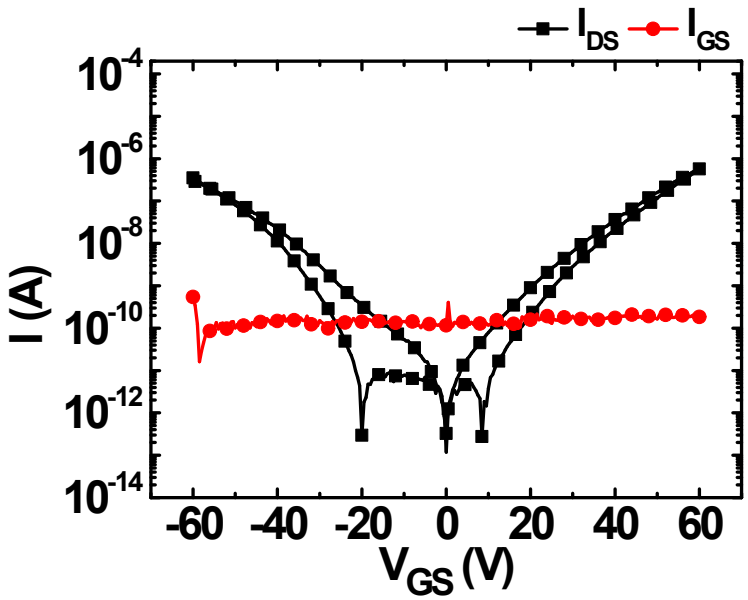

Figure S6. The source-drain current and the gate leakage current of the WSe_2 FET.

8. Thickness-dependent electrical conduction type of WSe_2 FETs

Table S1 summarize some previous studies of the thickness-dependent electrical conduction type for WSe_2 FETs. WSe_2 exhibits p-type for very thin thickness (< 4 nm), n-type for relatively thick thickness (> 26 nm), and ambipolar characteristics for intermediate thickness. Therefore we chose the Wse_2 flakes with 4-7 nm thickness to fabricate ambipolar FETs.

Table S1. The previous studies of thickness-dependent electrical conduction type of WSe_2 FETs

Thickness (nm)			Electrode	Remark
P-type	ambipolar	N-type		
<4	~ 6	>15	Ni/Au	Ref. [S1]
	7-26		Ti/Au	Ref. [S3]
	6		S: Ni, D: pd	Ref. [S4]
<3	~4	>5	Cr/Au	Ref. [S5]
	4 - 7		Ti/Au	This work

Reference

S1. C. Zhou, Y. Zhao, S. Raju, Y. Wang, Z. Lin, M. Chan and Y. Chai, Carrier Type Control of WSe_2 Field-Effect Transistors by Thickness Modulation and MoO_3 Layer Doping. *Adv. Funct. Mater.,* 2016, **26**, 4223-4230.

S2. J. F. Ziegler, M. D. Ziegler and J. P. Biersack, SRIM - The Stopping and Range of Ions in Matter (2010). *Nucl. Instrum. Methods Phys. Res. B,* 2010, **268**, 1818-1823.

S3. M. G. Stanford, M. G, P. R. Pudasaini, A. Belianinov, N. Cross, J. H. Noh, M. R. Koehler, D. G. Mandrus, G. Duscher, A. J. Rondinone and I. N. Ivanov, Focused helium-ion beam irradiation effects on electrical transport properties of few-layer WSe_2: enabling nanoscale direct write homo-junctions. *Sci. Rep.,* 2016, **6**. 27276.

S4. S. Das, and J. Appenzeller, WSe_2 field effect transistors with enhanced ambipolar characteristics. *Appl. Phys. Lett.,* 2013, **103**, 103501.

S5. P. R. Pudasaini, M. G. Stanford, A. Oyedele, A. T. Wong , A. N. Hoffman, D. P. Briggs, K. Xiao, D. G. Mandrus, T. Z. Ward and P. D. Rack, High performance top-gated multilayer WSe2 field effect transistors. *Nanotechnology* 2017, **28**, 475202.